Journal of Engineering Technology and Applied Physics

An Improved Backscattering Theoretical Model for Snow Area

Dina Naqiba Nur Ezzaty, Abd Wahid, Syabeela Syahali* and Muhamad Jalaluddin Jamri
Faculty of Engineering and Technology, Multimedia University, Jalan Ayer Keroh Lama, 75450 Melaka, Malaysia.
**Corresponding author: syabeela@mmu.edu.my*
https://doi.org/10.33093/jetap.2021.3.2.2
Manuscript Received: 25 February 2021, Accepted: 11 June 2021, Published: 15 December 2021

***Abstract* – Remote sensing has been studied for a long time to monitor the earth terrain. Remote sensing technology has been used globally in many different fields and one of the most popular area of study that uses remote sensing technology is snow monitoring. In previous researches, remote sensing has been modelled on snow area to study the scattering mechanisms of various scattering processes. In this paper, surface volume second order term that was dropped in previous study is derived, included and studied to observe the improvement in the surface volume backscattering coefficient. This new model is applied on snow layer above ground and the snow layer is modelled as a volume of ice particles as the Mie scatterers that are closely packed and bounded by irregular boundaries. Various parameters are used to investigate the improvement of adding the new term. Results show improvement in cross-polarized return, for all the range of parameters studied. Comparison is made with the field measurement result from U.S. Army Cold Regions Research and Engineering Laboratory (CRREL) in 1990. Close agreement is shown between developed model and data field backscattering coefficient result.**

Keywords* — *Surface volume scattering, remote sensing, theoretical modelling, backscattering coefficient, Radiative Transfer Equation.

I. Introduction

Remote sensing is a method of measuring the reflected and transmitted radiation at a distance to identify and monitor the physical features of an environment, typically from a satellite or an aircraft. The principle of radiative transfer (RT) explains how matter deals with electromagnetic radiation [1]. Remote sensing is a field of work that is closely correlated with RT. Remote sensing technology has been used globally in many different fields such as in agricultural crop monitoring to continuously monitor the growth stage of paddy field [3 - 5] or the growth and disease stage in oil palm field [6,7]. Remote sensing technology has also been used in climate change study such as in snow and sea ice monitoring in the polar region [8 - 11]. Apart from the examples given, many other fields also implement remote sensing technology. Since the Earth's surface can be observed repetitively by remote sensing systems various remote sensing methods for the agriculture areas, polar region [2,11 - 13], inland water [14] and others throughout the world, have been created.

A microwave signal from the radar system is transmitted to the area of concern and detects the signal scattered through the surface. When the electromagnetic wave is transmitted through a medium, there will be an interaction between them, requiring the modelling of surface-volume scattering, volume scattering and surface scattering. Surface volume scattering is the interaction between the scatterers and the surface or boundaries, volume scattering is the interaction among the scatterers and surface scattering is the interaction at the surfaces or boundaries of the layer [15 - 19].

An electrically dense medium backscattering model has been developed in [20]. The thick medium was modelled as a layer of homogeneous medium filled with a scattered dielectric spherical scatterrers, and bounded by rough surfaces on top and bottom of the layer. Owing to the dense medium phase and

Published by MMU PRESS. URL: https://journals.mmupress.com/index.php/jetap/index

amplitude correction theory (DM-PACT) [21], the near spacing effects of the scatterers were taken into account in the study of the modified phase matrix for the Mie scatterers. By applying radiative transfer equation, the backscattering coefficient was calculated [1]. Limited on the second order, the radiative transfer equation was solved. Volume scattering, surface volume scattering and surface scattering are the three key scattering mechanisms by referring to [22]. The Integral Equation Model (IEM) was used to model the top and bottom rough surfaces.

Study in [2] further enhanced the backscattering model by taking into account the scattering of the surface volume of second order. However, in the model developed by [2], many terms were disregarded during the second order surface volume scattering derivation as it was expected to have many losses. In this paper, the previously dropped term will be derived and included to investigate its significance in surface volume scattering contribution. The added term may give more accurate surface volume scattering return, hence, may be important and should not be ignored.

The modelling of the layer will be the first thing discussed in this paper, followed by model formulation, and a thorough analysis of surface volume backscattering return using various parameters.

II. THEORETICAL MODELLING

In this model, the second order surface volume scattering term which was dropped in the previous study [2] is included and analysed. In theoretical modelling, certain terms of second order surface volume scattering were considered in [2]. These terms are components of the iterative solution of the second order, derived from the radiative transfer equation solution second order. However, due to having comparatively higher losses, many terms in the second order iterative solution, which also define the process of second order surface volume scattering, were considered to be less important and were not taken into account in theoretical modelling. One of these terms is illustrated in Fig. 1.

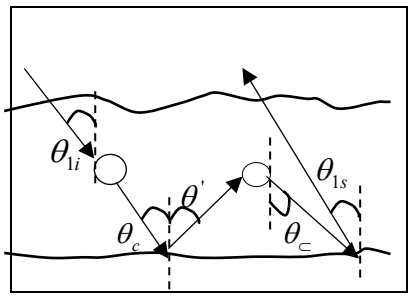

Fig. 1. Second order surface volume scattering term.

In this model, the second order surface volume scattering mechanism depicted in Fig. 1 which was previously dropped in [2] is derived and included as it also describes the second order surface volume scattering and may contribute to the total backscattering return. The newly derived second order surface volume scattering coefficient term illustrated in Fig. 1 is given by:

$$\sigma_{2pq}(\theta_s,\phi_s,\pi-\theta_i,\phi_i)$$

$$=\frac{\cos\theta_s}{4\pi}\sec\theta_{1s}T_{01}(\theta_s,\theta_{1s})T_{10}(\pi-\theta_{1i},\pi-\theta_i)$$

$$\int_0^{2\pi}\int_0^{\frac{\pi}{2}}\sec\theta_{\subset}\sin\theta_{\subset}d\theta_{\subset}d\phi_{\subset}$$

$$\int_0^{2\pi}\int_0^{\frac{\pi}{2}}\sec\theta_c\sin\theta_c d\theta_c d\phi_c$$

$$\int_0^{2\pi}\int_0^{\frac{\pi}{2}}\sec\theta'\sin\theta' d\theta' d\phi'$$

$$\sum_{t=v,hu=v,h}\sum_{v=v,h}P_{vq}(\pi-\theta_c,\phi_c,\pi-\theta_{1i},\phi_{1i})$$

$$P_{2tu}(\pi-\theta_{\subset},\phi_{\subset},\theta,\phi)$$

$$\sigma_{uv}(\theta',\phi',\pi-\theta_c,\phi_c)\sigma_{2pt}(\theta_{1s},\phi_{1s},\pi-\theta_{\subset},\phi_{\subset})$$

$$\left[\frac{L_{u^-}(\theta_c)-L_{q^-}(\theta_{1i})}{(ke_{q^-}\sec\theta_{1i}-ke_{u^-}\sec\theta_c)}\right]$$

$$\left[\frac{L_{u^+}(\theta')L_{u^-}(\theta_{\subset})-1}{-(ke_{u^+}\sec\theta'+ke_{u^-}\sec\theta_{\subset})}\right]L_{p^+}(\theta_{1s}) \quad (1)$$

θ_{1s} and θ_{1i} are the scattered angle and incident angle referring to Snell's Law. The propagation angles during the scattering process in the layer are represented by $\theta_c,\theta_{\subset}$ and θ' as shown in Fig. 1. p is the scattered field polarization while q is the incident field polarization. In the equation, u,v and t describe the field polarizations during the scattering process in the layer. T_{10} is the transmissivity from top boundary into the layer and T_{01} is the transmissivity from layer into the top boundary. P and P_2 are the phase matrix of the first and second scatterer respectively and L_u can be explained as the attenuation through the layer and is given by:

$$L_{u^{\pm}}(\theta)=e^{-keu^{\pm}\sec\theta(d)} \quad (2)$$

, where Ke is the volume extinction coefficient and u can be either vertical or horizontal polarization.

Equation (1) describes the movement and the scattering process in the layer for model in Fig. 1. The term defines the case where, as the first scatterer is hit by the downward intensity emitted through the upper

boundary and scattered to the lower boundary, the second scatterer is hit by the upward intensity reflected from the lower boundary. It also defines the situation where the scattered upward intensity from the lower boundary is scattered into downward intensity by the second scatterer before reaching the lower boundary and reflecting back to the upper boundary.

The improvement that this term may contribute in the surface volume backscattering return is studied and presented in the next section.

III. THEORETICAL ANALYSIS

To study the importance of the new term in surface volume scattering, the model is applied on a snow layer above ground. The snow layer is modelled as a volume of ice particles as the Mie scatterers that are closely packed and the layer is bounded by irregular boundaries. The ground is treated as a homogenous half space. The backscattering coefficient for surface volume scattering before adding the new term and after adding the new term is presented in the same graph for comparison purpose. The term 'Before' and 'After' in the graphs shown is referring to the pattern of the backscattering coefficient before and after adding the new term. Both results are included in order to observe the improvement on the surface volume backscattering coefficient after adding the new term.

Table I. Model Parameters Used in Theoretical Analysis of Snow Layer.

Parameters	Values used in Model
Frequency (GHz)	25
Scatterer Radius (mm)	0.5
Volume Fraction (%)	0.3
Effective relative permittivity of top layer	(1.0, 0)
Scatterer effective relative permittivity	(3.15, 0.015)
Background relative permittivity	(1.0, 0.0)
Lower half-space permittivity	(5.0, 0.0)
Thickness of layer (m)	1.0 m
Top surface rms height and correlation length (cm)	0.14 cm, 0.7 cm
Bottom surface rms height and correlation length (cm)	0.153 cm, 0.96 cm

The input parameters are set and listed in Table I. The backscattering coefficient for surface volume scattering is studied for frequency 25 GHz in a range of 10° to 50° incident angles. The effects of frequency, bottom surface roughness, volume fraction, scatterer effective relative permittivity and scatterer size on the improvement of surface volume backscattering coefficient due to the added term are investigated. The study is done by varying those parameters accordingly. The result and improvement of the backscattering coefficient for each parameter case is presented on a graph and analysed.

First, the model is analysed with various frequencies to study the improvement of surface volume backscattering coefficient after adding the new term. The frequency is varied from 25 GHz to 20 GHz and 23 GHz and the analysis is done by plotting the backscattering coefficient against incident angle from 10° to 50° for co-polarized and cross-polarized scattering process.

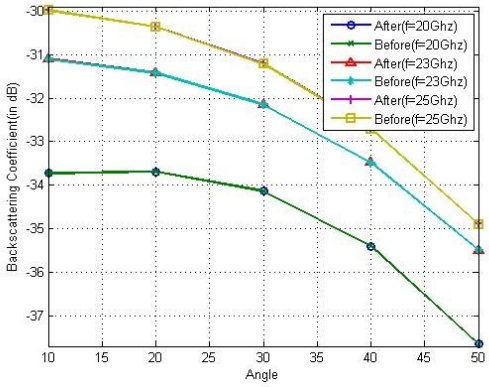

Fig. 2. Surface volume backscattering coefficient (VV polarization) against incident angle for various frequencies.

Based on Fig. 2, the new term does not give improvement for co-polarized. This is expected because second order surface volume scattering involves many scattering processes, hence contributes more on cross-polarized backscattering. Further study on this also shows that co-polarized backscattering is dominated by first order surface volume scattering compared to second order, as shown in Fig. 3. Hence, the added term which represents second order surface volume scattering is not important in co-polarized return.

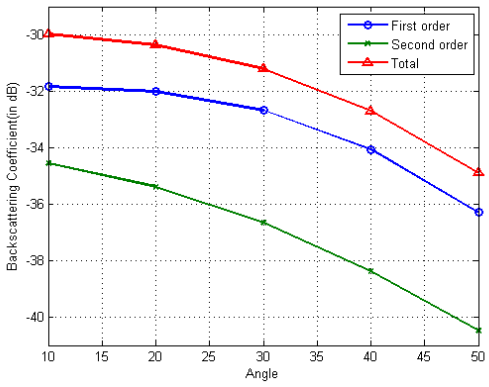

Fig. 3. Surface volume backscattering coefficient (VV) against incident angle at frequency of 25 GHz.

The effect of adding the new term in cross-polarization surface volume backscattering coefficient is clearly shown when various frequencies are plotted in the graph against incident angle for cross-polarized

(VH) scattering. In Fig. 4, improvement is seen for all the frequencies used although improvement is more in lower incident angle compared to higher incident angle. The reason may be that as incident angle increases, less wave reaches the bottom surface hence reducing the surface volume backscattering.

To study more on the improvement seen in Fig. 4, surface volume backscattering values are plotted for a larger range of frequencies from 15 GHz to 35 GHz.

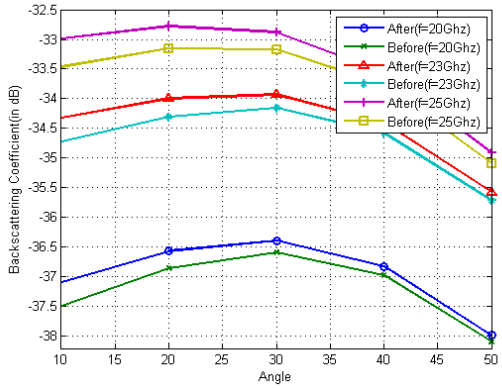

Fig. 4. Surface volume backscattering coefficient (VH polarization) against incident angle for various frequency.

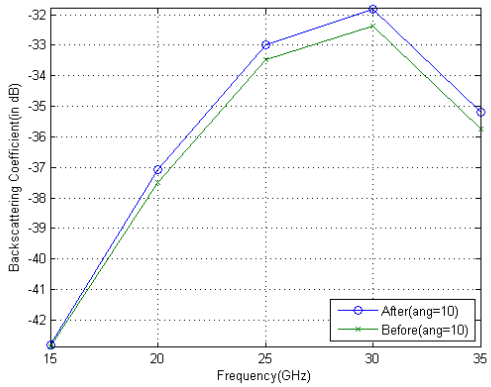

Fig. 5. Surface volume backscattering coefficient (VH polarization) against various frequency at 10 degree of incident angle.

It can be observed in Fig. 5 that the difference between the results before and after adding the new term is increasing as the frequency increases. This shows that the addition of the new term is more important at higher frequencies compared to lower frequencies. The backscattering coefficient increases as the frequency increases, because of higher albedo. However, the result also shows that as the frequency exceeds 30 GHz, the volume surface backscattering coefficient decreases rapidly, which indicates that at higher frequency above 30 GHz, the added term is no longer important.

Next, the bottom surface roughness of the snow-ground boundary is varied by changing its standard deviation of the surface height variation (RMS height), σ, normalized with frequency, kσ, where k is the wave number. In this simulation, kσ is varied from 0.8 to 1.0 and 1.2. The backscattering coefficient is plotted against incident angle. Same as in previous result, for co-polarized (VV) return, there is no improvement after adding the new term.

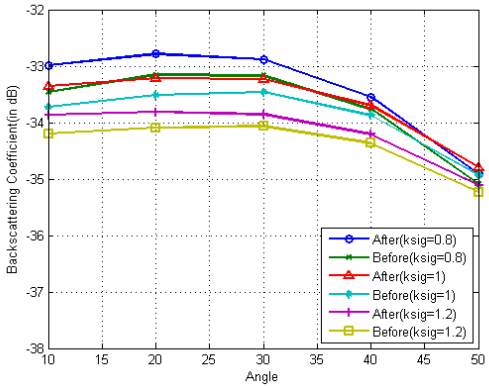

Fig. 6. Surface volume backscattering coefficient (VH polarization) against incident angle for various standard deviation of the surface height variation (RMS height) normalized with frequency, kσ.

In Fig. 6, the total backscattering coefficient for VH polarizations for different bottom surface kσ is plotted. There is quite significant difference in the result between previous model and the new model for all the kσ used, especially at lower incident angles. Therefore, adding the new term is important in cross-polarized scattering to improve the surface volume backscattering coefficient, for all the bottom surface roughness used.

Then, the volume fraction is varied from 0.3 to 0.4 and 0.5 to study its effect on the improvement of adding the new term. In the simulation, the backscattering coefficient is plotted against incident angle for VH polarized wave return for each volume fraction which are 0.3, 0.4 and 0.5.

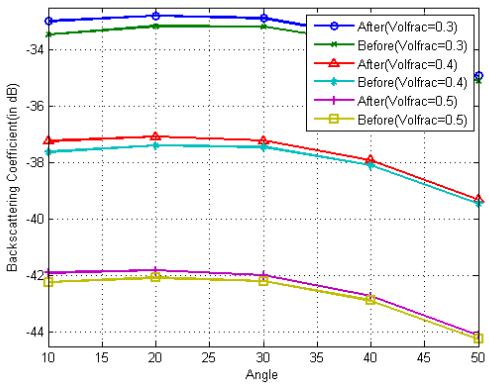

Fig. 7. Surface volume backscattering coefficient (VH polarization) against incident angle for various volume fraction.

In Fig. 7, it is shown that after adding the new term, the backscattering coefficient have improvement for all the volume fractions used. The backscattering coefficient after adding the new term is greater at lower incident angle and decreases as the incident

angle increases. Just like the previous results, no improvement is observed in co-polarized (VV) scattering for all the volume fraction used.

As the volume fraction increases, albedo is decreased, resulting in the decrease of the backscattering coefficient. This can be explained in [23] where it stated that volume fraction is a complex relationship between the coherence of scattering ensemble and number density of scatterers. Therefore, in lower volume fraction, the increase in albedo increases the value of backscattering coefficient for surface volume scattering.

After that, the improvement of backscattering coefficient after adding the new term for surface volume scattering is observed when the scatterer effective relative permittivity is changed. The scatterer effective relative permittivity is varied for the real part for 2, 3.15 and 4. The imaginary part is the same for all the results.

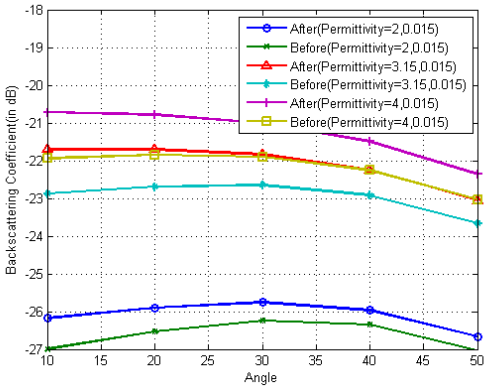

Fig. 8. Surface volume backscattering coefficient (VH polarization) against incident angle for various scatterer effective relative permittivity.

Figure 8 shows improvement in cross polarized return for all the permittivity used. It can also be observed that as the permittivity gets higher, the improvement gets bigger. Hence, the added term is more significant when the permittivity of scatterer is higher. As expected, the improvement of backscattering coefficient after adding new term is higher in lower incident angle compared to higher incident angle. No improvement can be seen on co-polarized scattering.

Lastly, the scatterer size also may affect the backscattering coefficient for surface volume scattering, hence the importance of the added second order surface volume scattering. To study on this matter, the size of the scatterer is changed accordingly from 0.5 mm to 0.4 mm and 0.6 mm scatterer radius.

In Fig. 9, the pattern of backscattering coefficient shows that in cross-polarized scattering, there is quite significant difference between the result before and after adding the new term, as the new model gives much effect on backscattering values for all the scatterer size used. Moreover, Fig. 9 also shows that the improvement is larger when the scatterer size is larger, hence the added term is more significant when the scatterer size is larger. As before, the improvement is more at lower incident angle compared to higher incident angle, and there is no improvement on co-polarized (VV) return.

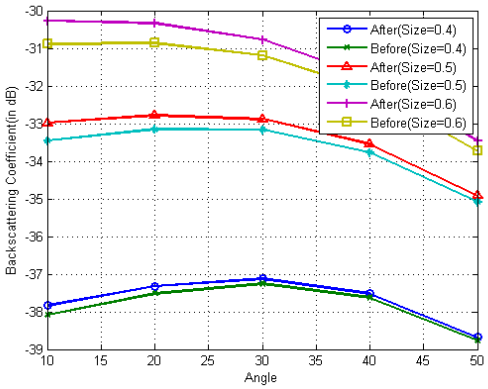

Fig. 9. Surface volume backscattering coefficient against incident angle for various scatterer radius.

IV. COMPARISON WITH FIELD MEASUREMENT

The new model developed in this study is compared with the field measurement result from the U.S. Army Cold Regions Research and Engineering Laboratory (CRREL) where the data was obtained during 1990 winters in Hanover, NH [24]. The measurement and characterization are presented in Table II.

Table II. Model Parameters Used in Comparison with Field Measurement.

Parameters	Values used in Model
Frequency (GHz)	18
Scatterer Radius (mm)	0.15
Volume Fraction (%)	0.6
Effective relative permittivity of top layer	(1.0, 0)
Scatterer effective relative permittivity	(1.0, 0)
Background relative permittivity	(3.3, 0.0001)
Lower half-space permittivity	(28.66, 37.07)
Thickness of layer (m)	0.3 m
Top surface rms height and correlation length (cm)	0.24 cm, 19.9 cm
Bottom surface rms height and correlation length (cm)	0.05 cm, 0.82 cm

By plotting HV polarized backscattering coefficient between CRREL'90 and the result from the model developed in this study, the comparison can be presented as in Fig. 10. Result shows promising match between the theoretical model and the measured data.

For the low incident angles, the gap is due to the feedthrough effects by the radar system as explained in [24].

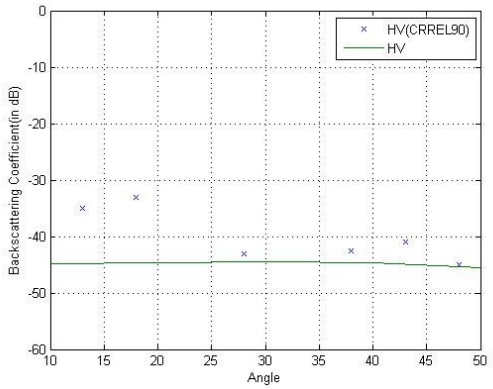

Fig. 10. Comparison between developed model and field measurement result from CRREL'90.

V. CONCLUSION

An improved backscattering theoretical model for snow area is proposed in this study, focusing on the surface volume scattering by adding the dropped term from the previous study [2]. The improvement can be clearly seen for cross polarized return for different values of input parameters which are frequency, bottom surface roughness, volume fraction, scatterer effective permittivity and scatterer radius used in this study. This new model is concluded to be important for cross polarized surface volume scattering calculation, especially in the area with larger scatterer size and permittivity, and when higher frequency range and lower incident angles are used. In future, numerical solution can be incorporated into this model to further improve the accuracy and widen the area of application of this model [25 - 29].

REFERENCES

[1] S. Chandrasekhar, "Radiative Transfer," *Dover Pub.*, New York, 1960.

[2] S. Syahali and H. T. Ewe, "Backscattering Analysis for Snow Remote Sensing Model With Higher Order of Surface-Volume Scattering," *Prog. in Electromagnet. Res.*, vol. 48, pp. 25-36, 2016.

[3] P. Kumara, R. Prasad, D. K. Gupta, A. K. Vishwakarma and A. Choudhary, "Retrieval of Rice Crop Growth Variables Using Multi-temporal RISAT-1 Remotely Sensed Data," *Russian Agric. Sci.*, vol. 43(6), pp. 461-465, 2017.

[4] T. C. Poh, K. J. Yi, L. K. Sing, S. Bahari, H. T. Ewe and H. T. Chuah, "Applications of Remote Sensing in The Monitoring of Rice Crops," *J. Inst. Eng. Malays*, vol. 67, pp. 2-11, 2006.

[5] P. Srikanth, A. Chakraborty and C. S. Murthy, "Crop Monitoring Using Microwave Remote Sensing," *Geospatial Techn. for Crops and Soils*, pp. 201-228, *Springer*, Singapore, 2021.

[6] C. M. Toh, H. T. Ewe, S. H. Tey and Y. H. Tay, "A Study on Oil Palm Remote Sensing at l-band With Dense Medium Microwave Backscattering Model," *IEEE Trans. on Geosci. and Remote Sensing*, vol. 57(10), pp. 8037-8047, 2019.

[7] K. C. Teng, J. Y. Koay, S. H. Tey, K. S. Lim, H. T. Ewe and H. T. Chuah, "A Dense Medium Microwave Backscattering Model for the Remote Sensing of Oil Palm," *IEEE Trans. on Geosci. and Remote Sensing*, vol. 53(6), pp. 3250-3259, 2014.

[8] C. T. Swift and D. J. Cavalieri, "Passive Microwave Remote Sensing for Sea Ice Research," *Eos, Trans. American Geophys. Union*, vol. 66(49), pp. 1210-1212, 1985.

[9] S. Syahali and H. T. Ewe, "Remote Sensing Backscattering Model for Sea Ice: Theoretical Modelling and Analysis," *Adv. in Polar Sci.*, vol. 24(4), pp. 258-264, 2013.

[10] S. Syahali and H. T. Ewe, "Model Development and Analysis of Multiple Surface Scattering and Surface-Volume Scattering in Sea Ice Layer," *IEEE Asia-Pacific Conf. on Appl. Electromagnet.*, pp. 22-27, 2012.

[11] S. Tan, J. Zhu, L. Tsang and S. V. Nghiem, "Full Wave Simulation of Snowpack Applied to Microwave Remote Sensing of Sea Ice," *IEEE Int. Geosci. and Remote Sensing Symp.*, 2017.

[12] J. Y. Koay, Y. J. Lee, H. T. Ewe and H. T. Chuah, "Electromagnetic Wave Scattering in Dense Media: Applications in the Remote Sensing of Sea Ice and Vegetation," *Electromagnet. Scattering: A Remote Sending Perspective*, pp. 303-339, 2017.

[13] J. Zhu, S. Tan, C. Xiong, L. Tsang, J. Lemmetyinen, C. Derksen and J. King, "Validation of Physical Model and Radar Retrieval Algorithm of Snow Water Equivalent Using Snow SAR Data," *IEEE Int. Geosci. and Remote Sensing Symp.*, pp. 322-325, 2017.

[14] G. Hu and L. Jia, "Monitoring of Evapotranspiration in A Semi-Arid Inland River Basin by Combining Microwave and Optical Remote Sensing Observations," *Remote Sensing*, vol. 7(3), pp, 3056-3087, 2015.

[15] Y. Yamaguchi, T. Moriyama, M. Ishido and H. Yamada, "Four-Component Scattering Model for Polarimetric SAR Image Decomposition," *IEEE Trans. on Geosci. and Remote Sensing*, vol. 43(8), pp. 1699-1706, 2005.

[16] P. B. Wei, M. Zhang, D. Nie and Y. C. Jiao, "Improvement of SSA Approach for Numerical Simulation of Sea Surface Scattering at High Microwave Bands," *Remote Sensing*, vol. 10(7), 1021, 2018.

[17] A. Sato, Y. Yamaguchi, G. Singh and S. E. Park, "Four-Component Scattering Power Decomposition with Extended Volume Scattering Model," *IEEE Geosci. and Remote Sensing Lett.*, vol. 9(2), pp, 166-170, 2011.

[18] L. Tsang, T. H. Liao, S. Tan, H. Huang, T. Qiao and K. H. Ding, "Rough Surface and Volume Scattering of Soil Surfaces, Ocean Surfaces, Snow, and Vegetation Based on Numerical Maxwell Model of 3-D Simulations," *IEEE J. Select. Topics in Appl. Earth Observations and Remote Sensing*, vol. 10(11), pp. 4703-4720, 2017.

[19] H. Bremmer, "Random Volume Scattering," *Radio Sci*, vol. 68(9), pp. 967-981, 1964.

[20] H. T. Ewe, H. T. Chuah and A. K. Fung, "A Backscatter Model for A Dense Discrete Medium: Analysis and Numerical Results," *Remote Sensing of Environ.*, vol. 65(2), pp. 195-203, 1998.

[21] A. K. Fung, S. Tsuatia, J. W. Bredow and H. T. Chuah, "Dense Medium Phase and Amplitude Correction Theory for Spatially and Electrically Dense Media," *1995 IEEE Int. Geosci. and Remote Sensing Symp., Quantitative Remote Sensing for Science and Applications*, vol. 2, pp. 1336-1338, 1995.

[22] A. K. Fung, "Microwave Scattering and Emission Models and Their Applications," *Artech House*, Massachusetts, 1994.

[23] D. G. Barber, A. K. Fung, T. C. Grenfell, S. V. Nghiem, R. G. Onstott, V. I. Lytle and A. J. Gow, "The Role of Snow on Microwave Emission and Scattering Over First-Year Sea Ice," *IEEE Trans. on Geosci. and Remote Sensing*, vol. 36(5), pp. 1750-1763, 1998

[24] S. Tjuatja, A. K. Fung and J. Bredow, "A Scattering Model for Snow Covered Sea Ice," *IEEE Trans. on Geosci. and Remote Sensing*, vol. 30(4), 1992.

[25] C. F. Lum, X. Fu, H. T. Ewe and L. J. Jiang, "A Study of Scattering from Snow Embedded with Non-Spherical Shapes of Scatterers with Relaxed Hierarchical Equivalent Source

Algorithm (RHESA)," *Prog. in Electromagnet. Res.,* vol. 61, pp. 51-60, 2017.

[26] X. Fu, L. J. Jiang and H. T. Ewe, "A Novel Relaxed Hierarchical Equivalent Source Algorithm (RHESA) for Electromagnetic Scattering Analysis of Dielectric Objects," *J. of Electromagnet. Waves and Appl.,* vol. 30, pp. 1631-1642, 2016.

[27] C. F. Lum, H. T. Ewe, F. Xin, L. J. Jiang and H. T. Chuah, "An Analysis of Scattering from Snow with Relaxed Hierachical Equivalent Source Algorithm," *2017 IEEE Int. Geosci. and Remote Sensing Symp.*, 2017.

[28] C. F. Lum, X. Fu, H. T. Ewe and L. J. Jiang, "A Study of Single Scattering of Scatterer at Various Orientation Angles with Equivalence Principle Algorithm," *2015 10th Int. Conf. on Inform., Comm. and Sign. Process.*, 2015.

[29] S. Syahali, H. T. Ewe, G. Vetharatnam, L. J. Jiang and H. A Kumaresan, "Backscattering Analysis of Cylinder Shaped Scatterer in Vegetation Medium: Comparison Between Theories," *J. Eng. Techn. and Appl. Phys.,* vol. 2, pp. 15-18, 2020.